

Isomerization and Dissociation of Ionized Dimethyl Sulfoxide: A Theoretical Insight

Guy Bouchoux,^{*,†,||} Hung Thanh Le,^{‡,§} and Minh Tho Nguyen^{‡,||}

Laboratoire des Mécanismes Réactionnels, UMR CNRS 7651, Ecole Polytechnique, F-91128 Palaiseau Cedex, France, Department of Chemistry, University of Leuven, Celestijnenlaan 200F, B-3001 Leuven, Belgium, and Group of Computational Chemistry, Faculty of Chemical Engineering, HoChiMinh-City University of Technology, Vietnam

Received: August 17, 2001; In Final Form: October 12, 2001

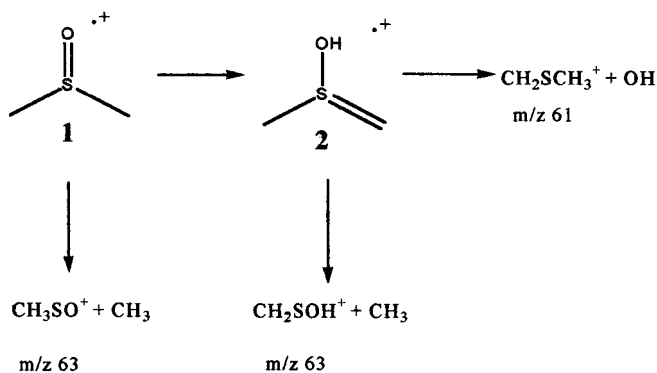
The potential energy profile associated with CH₃ and OH losses from the dimethyl sulfoxide radical cation, CH₃SOCH₃^{•+}, **1**, has been examined at the G2(MP2,SVP) level. Isomerization of **1** into its *aci*-tautomer, CH₃S(OH)CH₂^{•+}, **2**, by a 1,3-hydrogen migration constitutes the initial and energy-determining step of both dissociations. This explains the observation of identical appearance energies for the corresponding fragment ions. Heats of formation values of 702, 794, and 795 kJ/mol are obtained from atomization energies at the G2(MP2,SVP) level for CH₂SOH⁺, CH₃SO⁺, and CH₂SCH₃⁺, respectively. The kinetics of the reactions **2** → CH₂SCH₃⁺ + •OH and **2** → CH₂SOH⁺ + •CH₃ have been examined by using a RRKM-type orbiting transition state theory. Explicit consideration of the rotational effect is crucial, inducing the latter process to be dominant at a high internal energy of the precursor ions **2**. This offers the reason for why the *m/z* 63 (CH₂SOH⁺) ions are more abundant than the *m/z* 61 (CH₂SCH₃⁺) in the mass spectrum of dimethyl sulfoxide even though the OH loss represents the less energy demanding reaction.

1. Introduction

The electron impact mass spectrum of dimethyl sulfoxide (DMSO) presents four important peaks at *m/z* 78 (76%, M^{•+}), *m/z* 63 (100%, [M - CH₃]⁺), *m/z* 61 (17%, [M - OH]⁺), and *m/z* 45 (32%, HCS⁺).^{1,2} The losses of CH₃ and OH are the dominant fragmentations of the metastable ions produced following ionization of DMSO, and under this energy regime these two competitive reactions account for 95% of the fragment ions current and occur at almost identical rates.^{3,4} Concerning the [M - CH₃]⁺ (*m/z* 63) ions, collisional activation (CA) experiments demonstrate that two structures should be distinguished, namely, CH₃SO⁺ and CH₂SOH⁺.^{5,6} Moreover, the latter structure has been estimated, from molecular orbital calculations, to be ca. 100 kJ/mol less stable than the former.⁷ The [M - CH₃]⁺ ions coming from ionized DMSO in the metastable energy region correspond to the latter ion structure whereas, at higher energy, a mixture of both structures is produced.^{6,8} The experimental observations could be explained by the mechanistic pathways depicted in Scheme 1.

Accordingly, DMSO radical cation **1** may either eliminate a methyl radical to give CH₃SO⁺ or isomerize into its *aci*-tautomer **2**, which can further dissociate into CH₂SOH⁺ plus CH₃ or into CH₂SCH₃⁺ plus OH. The mass spectrum of metastable ions **2**, which presents two peaks at *m/z* 63 and *m/z* 61 in a ratio of 1/3,⁴ corroborates this view. The energetic aspect of the formation of [M - CH₃]⁺ and [M - OH]⁺ ions from DMSO has been explored by threshold photoelectron photoion coincidence mass spectrometry⁹ and the appearance energy of the [M - CH₃]⁺ ions has been used to derive the heat of formation of CH₂SOH⁺.^{7,9} Similarly, the appearance energy of [M - OH]⁺

SCHEME 1



ions has been used to derive the heat of formation of CH₂SCH₃⁺.⁹ However, the theoretical investigation of Gozzo and Eberlin⁸ suggested that the heat of formation of CH₂SOH⁺ and CH₂SCH₃⁺ ions could not be related to their appearance energy value since the isomerization barrier **1** → **2** (Scheme 1) is seemingly higher than the dissociation products. This point is of crucial interest not only for the determination of the heat of formation of CH₂SOH⁺ and CH₂SCH₃⁺ ions, but also for that of the sulfine molecule CH₂SO. As a matter of fact, the heat of formation of CH₂SOH⁺ ions can be combined with the experimental value of the gas-phase basicity of the sulfine molecule^{10,11} to derive Δ_fH^o (CH₂SO). In connection with this question, it should be emphasized that the currently available theoretical estimates of Δ_fH^o (CH₂SO) lie in a very large range extending from -3 ± 14¹² to -52 ± 10 kJ/mol,¹³ which reasonably thus justifies another mean of determination of these quantities.

The present study is intended to provide a more accurate estimate of the energies involved during the reactions presented in Scheme 1, particularly the isomerization step **1** → **2**. For this purpose we used ab initio molecular orbital calculations

[†] Ecole Polytechnique.

[‡] University of Leuven.

[§] HoChiMinh-City University of Technology.

^{||} E-mails: bouchoux@dcmr.polytechnique.fr, minh.nguyen@chem.kuleuven.ac.be.

up to the G2 level. Subsequently, a RRKM-type statistical treatment of the reaction rates is also carried out in order to understand the kinetics of the dissociative processes of low energy ions **1** and **2**.

2. Theoretical Methods

All ab initio quantum chemical calculations were performed by using the Gaussian 98 set of programs.¹⁴ The system examined here has been studied using both correlated molecular orbital and density functional theory methods. In the former approach, the geometries of the different species investigated were first optimized at the HF/6-31G(d) level within the unrestricted formalism (UHF); the zero point energy (ZPE) has been calculated at this level after scaling by a factor of 0.8929. The geometries were then refined at the MP2/6-31G* level to take electron correlation effects explicitly into account. It has been established that accurate heats of formation (i.e., ± 6 kJ/mol) can be obtained from calculations at the G2 level of theory or its variants, G2(MP2) and G2(MP2,SVP).¹⁵ For the present investigation, we used the G2(MP2,SVP) technique, in this approach, the energies are calculated at the QCISD(T) level using the split-valence plus polarization (SVP) 6-31G(d) basis set. Corrections for basis set deficiencies are evaluated at the MP2/6-311+G(3df,2p) level. A higher-level correction (HLC), which depends on the number of paired and unpaired electrons, is finally introduced. The total energy $E[\text{G2}(\text{MP2},\text{SVP})]$ is then given by

$$E[\text{G2}(\text{MP2},\text{SVP})] = E[\text{QCISD}(\text{T})/6-31\text{G}(\text{d})] + E[\text{MP2}/6-311+\text{G}(3\text{df},2\text{p})] - E[\text{MP2}/6-31\text{G}(\text{d})] + \text{HLC} + \text{ZPE}$$

The HLC correction is calculated from $\text{HLC} = -An_\beta - Bn_\alpha$, with n_β and n_α being the number of β and α valence electrons respectively ($n_\beta < n_\alpha$), and the parameters A and B equal 5.13×10^{-3} and 0.19×10^{-3} hartree, respectively.

It is known that density functional theory may provide accurate results at a less expensive cost. For the sake of comparison with G2(MP2,SVP) results, optimized geometries and zero-point energy corrections (ZPE) to relative energies were obtained using DFT with the popular B3LYP functional and the 6-311++G(d,p) basis set.

3. Results and Discussion

Potential Energy Profile. The potential energy profile associated with Scheme 1 has been previously investigated by Gozzo and Eberlin⁸ at the (U)MP2/6-31G(d,p)+ZPE level of theory. These authors found that structure **1** is less stable than **2** by 29 kJ/mol and that a significant energy barrier (128 kJ/mol) is associated with the isomerization **1** \rightarrow **2**. This places the corresponding transition structure above the dissociation products $\text{CH}_2\text{SOH}^+ + \text{CH}_3$ and $\text{CH}_2\text{SCH}_3^+ + \text{OH}$ by 15 and 51 kJ/mol, respectively.

The results of our exploration of this system at the MP2/6-311++G(d,p)+ZPE, B3LYP/6-311++G(d,p)+ZPE and G2-(MP2,SVP) levels are summarized in Table 1, and the geometrical parameters of the relevant structures are presented in Figure 1.

Both the G2(MP2,SVP) and B3LYP + ZPE results agree with each other in placing structure **1** below structure **2** by ca. 20 kJ/mol while the energy barrier **1** \rightarrow **2** is situated in the range 150–170 kJ/mol. Most importantly, it is confirmed that this isomerization barrier lies above the dissociation products by at least 25 kJ/mol for the methyl loss and 45 kJ/mol for the OH

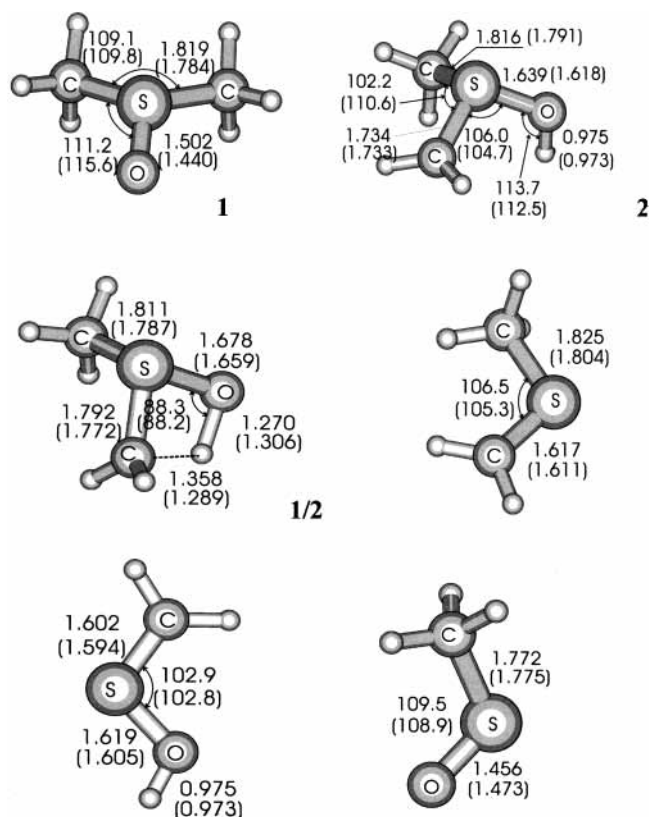


Figure 1. Optimized geometrical parameters obtained at the B3LYP/6-311++G(d,p) level (into parentheses: MP2/6-311++G(d,p) results) for ionized DMSO, **1**, its aci-tautomer, **2**, and the $[\text{M} - \text{OH}]^+$ and $[\text{M} - \text{CH}_3]^+$ fragment ions.

TABLE 1: Calculated Relative Energies Including Zero Point Corrections (kJ/mol)

structures	MP2 ^a	B3LYP ^a	
	6-311++G(d,p)	6-311++G(d,p)	G2(MP2,SVP)
$\text{H}_3\text{C}-(\text{SO})\text{CH}_3$ (1)	0.0	0.0	0.0
$\text{H}_2\text{C}-\text{S}(\text{OH})\text{CH}_3$ (2)	-11.6	19.1	23.0
TS 1/2	139.9	151.1	168.4
$\text{H}_2\text{C}=\text{S}-\text{CH}_3^+ + \text{OH}$	48.9	85.9	122.9
$\text{H}_2\text{C}=\text{S}-\text{OH}^+ + \text{CH}_3$	97.5	127.1	137.6
$\text{CH}_3\text{SO}^+ + \text{CH}_3$	172.9	227.4	230.4

^a ZPE obtained from MP2/6-31G(d,p) calculations scaled by a factor 0.95.

loss. To determine whether the step **1** \rightarrow **2** is really the energy-determining step for dissociation of ions **1**, we attempted to locate the transition structures associated with the methyl and hydroxyl losses from **2**. At the UHF/6-31G(d) level, two transition structures were found and characterized by one negative eigenvalue in their force constant matrixes. Nevertheless, it turns out that at a higher level of theory, the energies of these structures were situated well below that of the separated products. All tentative calculations at the MP2/6-31G++(d,p) or B3LYP/6-311++G(d,p) levels invariably led to similar failure of a transition structure determination. Such a situation is often encountered for reactions occurring on a continuously endothermic potential energy surface, i.e., through a loose transition state. This is precisely what is expected for the two considered reactions, **2** \rightarrow $\text{CH}_2\text{SOH}^+ + \text{CH}_3$ and **2** \rightarrow $\text{CH}_2\text{SCH}_3^+ + \text{OH}$, which involve simple C-C and C-O bond elongation. As a consequence, we could reasonably conclude that both dissociations do not involve any reverse energy barrier. A comparable situation is also encountered for the direct methyl

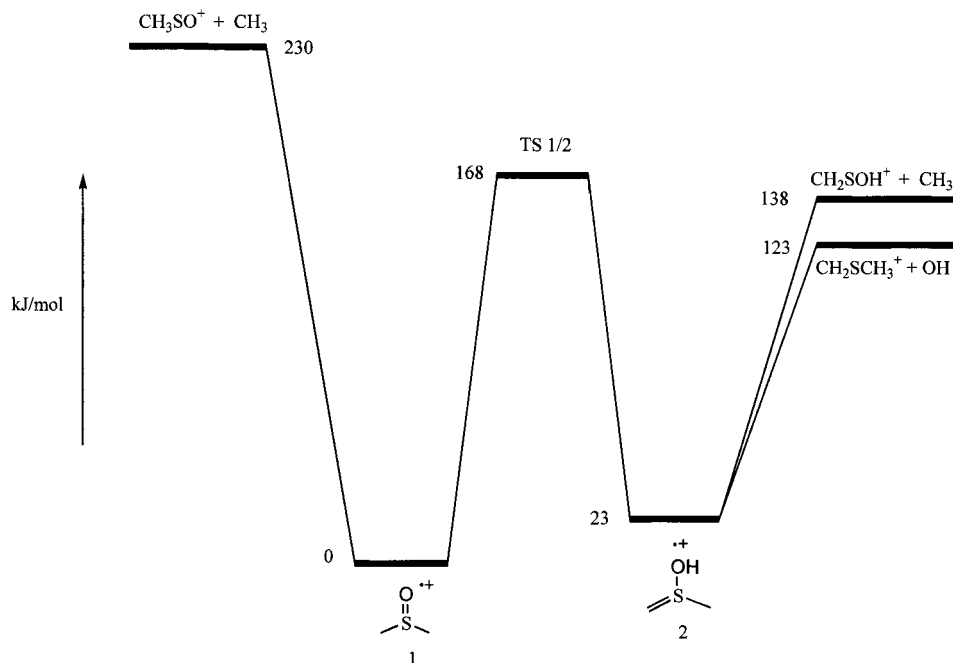


Figure 2. G2(MP2,SVP) 0 K energy profile for the isomerization/dissociation of ionized DMSO.

loss from ionized DMSO to give $\text{CH}_3\text{SO}^+ + \text{CH}_3$. Figure 2 summarizes these results in terms of 0 K energy profile.

It is obvious from this figure that ionized DMSO **1** should overcome an isomerization barrier $1 \rightarrow 2$ higher in energy than that required by the fragmentation of **2**. This view is corroborated by experimental observations. Accordingly, the appearance energies of $[\text{M} - \text{CH}_3]^+$ and $[\text{M} - \text{OH}]^+$ ions from DMSO are equal to 10.64 ± 0.07 and 10.55 ± 0.07 eV, respectively.⁹ If we take the experimental errors into account, these two values are essentially identical and it strongly suggests that the experimental appearance energies are associated with a common energy determining step, presumably $1 \rightarrow 2$. Using a mean value of 10.6 eV for this common appearance energy and 9.10 eV for the ionization energy of DMSO (value obtained from photoionization experiments¹⁶), we derive an apparent energy barrier of $145 (\pm 20)$ kJ/mol. It is noted that this value is satisfactorily close to the critical energy calculated for the reaction $1 \rightarrow 2$ (140–169 kJ/mol, Table 1).

The second interesting result provided by the calculations is the energy ordering of the dissociation products. At all the theoretical levels examined here, the set of products $\text{CH}_2\text{SCH}_3^+ + \text{OH}$ is situated below $\text{CH}_2\text{SOH}^+ + \text{CH}_3$. The difference amounts to 15–40 kJ/mol depending upon the level of theory. This is in line with the observation that metastable ions **2** dissociate mainly by OH loss.⁴ What is less easily explainable is the fact that the methyl loss becomes more important for ions **1** of low internal energy. For example, metastable ions **1** eliminate OH or CH_3 at identical rates.^{3,4} Moreover, during PEPICO experiments on DMSO, Meisels et al.⁹ observed that the methyl loss always overcomes the OH loss in the photon energy range 9.0–17.0 eV. Part of the observations is obviously due to the opening of the second dissociation route leading to $\text{CH}_3\text{SO}^+ + \text{CH}_3$. This latter set of products is predicted to lie 230 kJ/mol above **1** at both G2(MP2,SVP) and B3LYP/6-311++G(d,p) levels. However, the predominant loss of a methyl group from ions **1** is still observed below the threshold for this higher energy process.⁹ This aspect will be discussed in conjunction with statistical rate constant calculations in a second section.

Before entering into the kinetic aspect of the dissociations of ions **1** and **2**, it is of interest to make a brief comment on the thermochemistry of ions $\text{CH}_2\text{SCH}_3^+$, CH_2SOH^+ , and CH_3SO^+ . Using the experimental appearance energies of 10.64 ± 0.07 and 10.55 ± 0.07 eV for $[\text{M} - \text{CH}_3]^+$ and $[\text{M} - \text{OH}]^+$ ions from DMSO⁹ and $\Delta_f H^\circ$ values of -150.5 , 147, and 39 kJ/mol for DMSO, CH_3 , and OH, respectively,¹⁶ we can derive the “apparent” heats of formations of 729 ± 8 and 828 ± 8 kJ/mol for CH_2SOH^+ and $\text{CH}_2\text{SCH}_3^+$ ions. The former value is slightly at variance from the original proposal by Meisel et al.⁹ (736 kJ/mol) probably because a new value of the heat of formation of the methyl radical is used here. We can also confirm the correct assignment of the $[\text{M} - \text{CH}_3]^+$ structure to be CH_2SOH^+ ,^{6,7} not CH_3SO^+ as originally assumed.⁹ However, it appears clearly from examination of the present data (Table 1, Figure 2) that the “apparent” heats of formation of ions CH_2SOH^+ and $\text{CH}_2\text{SCH}_3^+$ are substantially overestimated values of the true heats of formation. Clearly, other experiments have to be designed in order to obtain correct experimental $\Delta_f H^\circ$ values for CH_2SOH^+ and $\text{CH}_2\text{SCH}_3^+$ ions. In the absence of such experiments, a theoretical estimate can be done using the G2(MP2,SVP) atomization energies.¹⁷ As recalled in the computational section, this method provides generally heats of formation values that are close to the experimental ones within ± 6 kJ/mol.¹⁵ We obtain here: $\Delta_f H_{298}^\circ [\text{CH}_2\text{SOH}^+] = 702$ kJ/mol and $\Delta_f H_{298}^\circ [\text{CH}_2\text{SCH}_3^+] = 795$ kJ/mol, suggesting significant downward revision of the currently used values (736^{6,7} and 812 kJ/mol,¹⁶ respectively). Similarly, a value of 794 kJ/mol is calculated for the 298 K heat of formation of CH_3SO^+ ions. It confirms the previously suspected large difference in enthalpy between the two isomeric ions CH_2SOH^+ and CH_3SO^+ .^{6–8}

Kinetic Treatment. For two competitive reactions occurring via structurally similar transition states, it is commonly accepted that the rate constant associated with the lowest critical energy process will be dominant at all internal energy. This is what would be expected for the two dissociation channels $2 \rightarrow \text{CH}_2\text{SOH}^+ + \text{CH}_3$ and $2 \rightarrow \text{CH}_2\text{SCH}_3^+ + \text{OH}$, since they proceed via loose transition structures. In this simple

TABLE 2: Parameters Used in the Orbiting Transition State Calculations^a

species	frequencies (cm ⁻¹)						rotational constant (cm ⁻¹)	polarizability (Å ³)	dipole moment (Debye)
1	137	167	243	273	316	609	0.19		
	715	888	924	941	1017	1179			
	1307	1334	1379	1385	1392	1403			
	2932	2934	3053	3054	3067	3069			
	103	197	262	278	320	393			
	532	672	772	796	898	963			
2	1009	1146	1332	1372	1404	1410	0.19		
	2941	3053	3056	3071	3197	3497			
	688	176	256	289	425	586			
	1032	706	830	902	952	1002			
TS1/2	1863	1124	1330	1351	1391	1408	0.19		
	2936	3001	3050	3068	3134	3134			
CH ₂ SOH ⁺	30	353	660	814	921	1010	0.42		
	1027	1170	1412	2983	3098	3561			
CH ₃	276	1378	1378	2940	3098	3098	7.7	1.4	0.0
	40	320	567	634	915	989			
CH ₂ SCH ₃ ⁺	994	1046	1056	1359	1410	1432	0.35		
	1450	2909	2995	3004	3017	3102			
OH	3576						19.3	0.54	1.8

^a Obtained from HF/6-31G(d) optimized geometries; vibrational frequencies are scaled by a factor 0.895; the rotational constants are in fact the geometric means of their components.

view, the OH elimination would always dominate over the CH₃ loss since the associated critical energies amount respectively to 1.04 and 1.19 eV for both processes (G2(MP2,SVP) results, Table 1). This is true for metastable ions **2** but contrary to the experimental observations if **2** is collisionally activated⁴ or produced from isomerization of **1**.^{1-4,9} In these cases, on the contrary, the CH₃ loss predominates over the OH elimination. It is no doubt that a rigorous statistical treatment of the kinetic of the reaction involving simple bond elongations should be considered in order to understand the experimental observations, and this point will be examined in some details in the following lines.

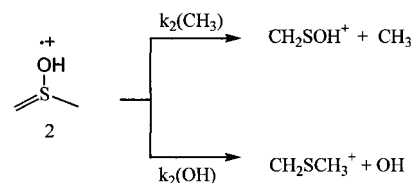
The dissociation rate constant of an ion of internal energy E and angular momentum J is given by (eq 1)

$$k(E) = N^\ddagger(E-E_0, J) / h\rho(E, J) \quad (1)$$

where $N^\ddagger(E-E_0, J)$ is the sum of state of the transition structure, E_0 is the critical energy of the dissociation, $\rho(E, J)$ is the density of state of the reactant ion, and h is Planck's constant. When a reaction path has no energy barrier, its description in terms of a single transition state becomes a difficult task, simply because the position of the latter along the reaction path is not known. However, different methods for treating these situations have been developed, among them the variational transition state model¹⁸ and the orbiting transition state model.¹⁹ The former is based on the idea that the transition structure is located where N^\ddagger is a minimum. The location of this variational transition state depends on the total energy E and on the potential energy function associated with the dissociation. Several methods have been proposed to find this transition state but, generally, the amount of effort is considerable if a good accuracy is desired. Moreover, additional complications arise when the rotational motion of the products have to be imperatively taken into account in the kinetic analyses.¹⁸

The orbiting transition state model is based on the "phase space theory" hypothesis that the statistical dissociation rate constant can be calculated from the characteristics of the reverse reaction by assuming strict conservation of energy and angular momentum. The orbiting transition structure is located at the maximum of an "effective" potential energy curve. This latter is the sum of the classical potential energy functions, as usually

SCHEME 2



described, for example, by a Morse or a Lennard-Jones function, and the centrifugal potential, which is always positive and monotonically vanishing at large internuclear separation. The position of this maximum is only dependent on the angular momentum and on the curvature of the long range attractive potential, which is a function of the reduced mass of the fragments and of the polarizability of the departing neutral fragments. This model takes explicitly into account the conservation of the angular momentum by assuming that the orbital rotational energy of the orbiting transition state is converted into relative translational energy of the products. The rate constant is calculated by evaluating the term $N^\ddagger(E-E_0, J)$ (eq 1) by a convolution of the rotational sum of states of the products (the function Γ in ref 19) and their density of vibrational states. The cornerstone of the orbiting transition state model is the function Γ , for which the various forms, for several combinations of products, have been tabulated.¹⁹

The use of the orbiting transition state model needs only the knowledge of the geometrical parameters and the frequencies of the reactant and the products. In the present study, this method has been applied to the two competitive dissociation channels of ions **2** (Scheme 2).

Calculations of the rate constants $k_2(\text{CH}_3)$ and $k_2(\text{OH})$ were performed using the statistical theory package elaborated by Chesnavich et al.²⁰ The parameters used in the calculations are gathered in Table 2; the critical energies are those estimated ab initio at the G2(MP2,SVP) level. The resulting rate constant curves, as a function of the internal energy of ions **2**, E' , are displayed in Figure 3. A 298 K Maxwell-Boltzmann distribution of precursor ions **2** has been assumed during the calculations.

From an examination of Figure 3 it appears that, at low internal energy, ions **2** eliminate more readily the OH group than the CH₃ group. This was obviously expected from the

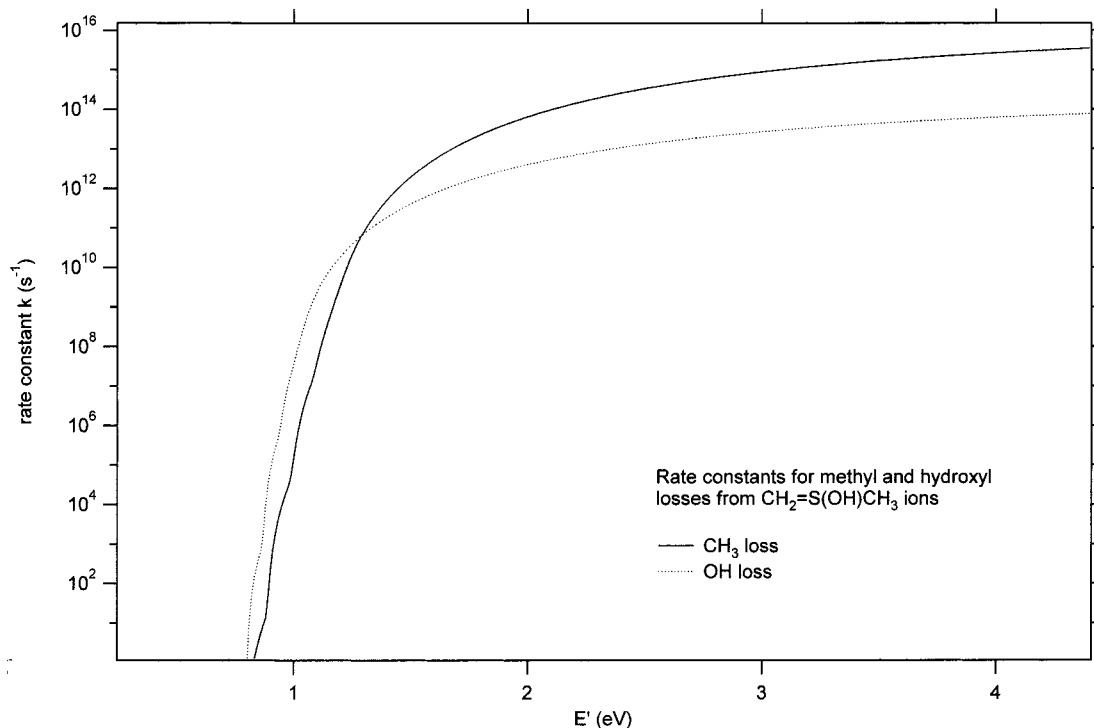


Figure 3. Calculated orbiting transition state rate constants for elimination of CH_3 or OH from ionized *aci*-DMSO, **2**. Parameters used in the computations are gathered in Table 2, the critical energy for the two processes were obtained at the G2(MP2,SVP) level (1.43 and 1.27 eV, respectively).

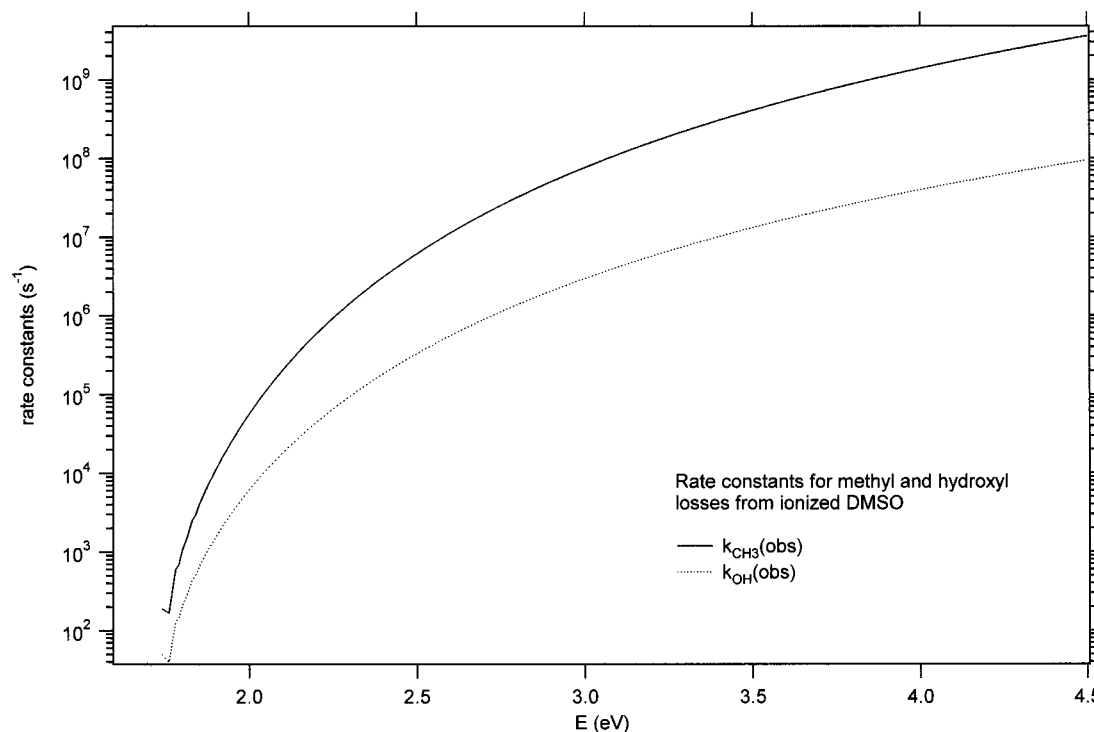


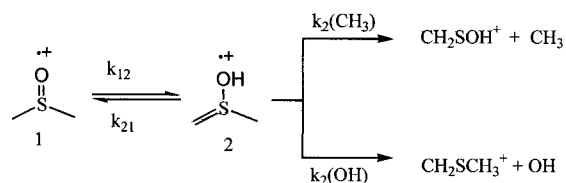
Figure 4. Calculated orbiting transition state rate constants for elimination of CH_3 or OH from ionized DMSO, **1**. Parameters used in the computations are gathered in Table 2, the common threshold for the two processes corresponds to the energy determining step $1 \rightarrow 2$ (1.75 eV at the G2(MP2,SVP) level).

relative critical energies of both processes. It is worth noting that the ordering of the rate constants, $k_2(\text{CH}_3) < k_2(\text{OH})$, applies in the metastable region (i.e., for k values near 10^5 s^{-1}) in agreement with the experiments. By contrast, at high internal energy, Figure 3 indicates that the rate constant $k_2(\text{CH}_3)$ becomes largely dominant over $k_2(\text{OH})$. This result, also in agreement with experimental observations, but surprising in view of the

fact that the CH_3 loss possesses the largest critical energy, deserves some comments.

As indicated above, complete expressions of the sum of rotational states Γ used to derive the rate constant values $k(E, J)$ are given in ref 19. From these expressions, the role of the rotational energy E_{rot} and of the nature of the dissociation products on the sum of rotational states between zero and E_{rot} ,

SCHEME 3



Γ , can qualitatively be understood. Accordingly, Γ is (i) proportional to $(E_{\text{rot}})^{s/2}$, where s is the total number of rotational degrees of freedom of the pair of products, and (ii) inversely proportional to the product $(A)^{a/2}(B)^{b/2}$, where A and B are the rotational constants of the products and a and b are their individual rotational degrees of freedom. It follows that, if the number s is large, as for example for a sphere–sphere pair of products ($s = 6$), the sum Γ is large and also the rate constant $k(E, J)$. Considering the two competing reactions, $2 \rightarrow \text{CH}_2\text{SOH}^+ + \text{CH}_3$ and $2 \rightarrow \text{CH}_2\text{SCH}_3^+ + \text{OH}$, while the former may be described as a sphere–sphere dissociating system ($s = 6$), the latter is obviously a sphere–linear system ($s = 5$). The difference in s values leads to an expectation that the methyl loss will occur at a higher rate than the OH loss, simply due to a higher number of rotational levels in the transition state. Furthermore, the rotational constants also play a significant role in the present competition. From the MP2/6-31G(d) optimized geometries it appears that the rotational constants for CH_2SOH^+ and $\text{CH}_2\text{SCH}_3^+$ are approximately the same ($\sim 0.4 \text{ cm}^{-1}$, Table 2) but for CH_3 and OH the values are clearly different (8 and 19 cm^{-1} , respectively, Table 2). This difference also contributes to a greater rate constant for the methyl loss than for the OH elimination. The calculations reveal that both effects contribute similarly to the difference in rate constant, which attains about 2 orders of magnitude at high internal energy E' . Finally, we note that the difference in polarizability between the two departing neutral fragments does not play, in the present case, a significant role in the rate constant differences.

The behavior of low energy ionized DMSO, **1**, may be described by assuming the simple kinetic scheme associated with Scheme 3.

Assuming the steady-state approximation to the intermediate ions **2**, the apparent rate constants for CH_3 and OH losses from **1**, $k_{1\text{obs}}(\text{CH}_3)$ and $k_{1\text{obs}}(\text{OH})$, may be expressed by $k_{1\text{obs}}(\text{CH}_3) = Kk_2(\text{CH}_3)$ and $k_{1\text{obs}}(\text{OH}) = Kk_2(\text{OH})$ with $K = k_{12}/[k_{12} + k_{21} + k_2(\text{OH}) + k_2(\text{CH}_3)]$. Using the parameters presented in Table 2 for the calculation of each individual reaction rates as a function of the internal energy of ions **1**, E , we obtain the results illustrated by Figure 4.

Since the critical energy for the isomerization $1 \rightarrow 2$ (1.75 eV) is higher than the crossing energy of the two $k(E')$ curves (Figure 3), it is not surprising to find that $k_{1\text{obs}}(\text{CH}_3)$ is always greater than $k_{1\text{obs}}(\text{OH})$. Moreover, the data in Figure 4 show that slow effect of the $1 \rightarrow 2$ barrier is responsible of the observation of metastable dissociations from **1** (i.e., reactions occurring with a rate constant close to 10^5 s^{-1}).

4. Concluding Remarks

In conclusion, the present work confirms that the low energy dissociation processes of ionized DMSO **1** are preceded by an energy-determining isomerization into its *aci*-isomer **2**. This

renders the use of the appearance energies of the corresponding ions to derive their heats of formation erroneous. New estimates are proposed for these quantities on the basis of G2(MP2,SVP) atomization energies. A detailed kinetic treatment of the dissociation of both ions **1** and **2** shows that a competition between the two inherent bond cleavages is not only governed by their respective critical energies but also by the rotational effects that may induce far reaching incidences on the rate constants, especially at high internal energy. This consideration affords a satisfactory rationalization of the mass spectra of DMSO and its *aci*-isomer previously observed under different conditions.

Acknowledgment. We thank the CNRS and Government of the Flemish Community of Belgium for supporting a bilateral cooperation project. The Leuven group is grateful to the KULeuven research council for financial support (GOA program).

References and Notes

- (1) Bowie, J. H.; Williams, D. H.; Lawesson, S. O.; Madsen, J. O.; Nolde, C.; Schroll, G. *Tetrahedron* **1966**, *22*, 3515.
- (2) Smakman, R.; de Boer, Th. J. *Org. Mass Spectrom.* **1970**, *3*, 1561.
- (3) Griffith, I. W.; Howe, I.; March, R.; Beynon, J. H. *Int. J. Mass Spectrom. Ion Processes* **1983**, *54*, 323.
- (4) Carlsen, L.; Egsgaard, H. *J. Am. Chem. Soc.* **1988**, *110*, 6701.
- (5) Turecek, F.; Drinkwater, D. E.; McLafferty, F. W. *J. Am. Chem. Soc.* **1989**, *111*, 7696.
- (6) McGibbon, G. A.; Burgers, P. C.; Terlouw, J. K. *Chem. Phys. Lett.* **1994**, *218*, 499.
- (7) Ruttink, P. J. A.; Burgers, P. C.; Terlouw, J. K. *Chem. Phys. Lett.* **1994**, *229*, 495.
- (8) Gozzo, F. C.; Eberlin, M. N. *J. Mass Spectrom.* **1995**, *30*, 1553.
- (9) Zha, Q.; Nishimura, T.; Meisels, G. G. *Int. J. Mass Spectrom. Ion Processes* **1988**, *83*, 1.
- (10) Bouchoux, G.; Salpin, J.-Y. *J. Am. Chem. Soc.* **1996**, *118*, 6516.
- (11) Bouchoux, G.; Salpin, J.-Y. *Rapid Commun. Mass Spectrom.* **1999**, *13*, 932.
- (12) Ruttink, P. J. A.; Burgers, P. C.; Francis, J. T.; Terlouw, J. K. *J. Phys. Chem.* **1996**, *100*, 9694.
- (13) (a) Ventura, O. N.; Kieninger, M.; Cachau, R.; Suhai, S. *Chem. Phys. Lett.* **2000**, *329*, 145. (b) Ruttink, P. J. A.; Burgers, P. C.; Trikoupi, M. A.; Terlouw, J. K. *Chem. Phys. Lett.* **2001**, *342*, 447. (c) Heydorn, L. N.; Ling, Y.; De Oliveira, G.; Martin, J. M. L.; Lifshitz, C.; Terlouw, J. K. *Z. Phys. Chem.* **2001**, *215*, 141.
- (14) Frisch, M. J.; Trucks, G. W.; Schlegel, H. B.; Scuseria, G. E.; Robb, M. A.; Cheeseman, J. R.; Zakrzewski, V. G.; Montgomery, J. A., Jr.; Stratmann, R. E.; Burant, J. C.; Dapprich, S.; Millam, J. M.; Daniels, A. D.; Kudin, K. N.; Strain, M. C.; Farkas, O.; Tomasi, J.; Barone, V.; Cossi, M.; Cammi, R.; Mennucci, B.; Pomelli, C.; Adamo, C.; Clifford, S.; Ochterski, J.; Petersson, G. A.; Ayala, P. Y.; Cui, Q.; Morokuma, K.; Malick, D. K.; Rabuck, A. D.; Raghavachari, K.; Foresman, J. B.; Cioslowski, J.; Ortiz, J. V.; Stefanov, B. B.; Liu, G.; Liashenko, A.; Piskorz, P.; Komaromi, I.; Gomperts, R.; Martin, R. L.; Fox, D. J.; Keith, T.; Al-Laham, M. A.; Peng, C. Y.; Nanayakkara, A.; Gonzalez, C.; Challacombe, M.; Gill, P. M. W.; Johnson, B. G.; Chen, W.; Wong, M. W.; Andres, J. L.; Head-Gordon, M.; Replogle, E. S.; Pople, J. A. *Gaussian 98*, revision A.6; Gaussian, Inc.: Pittsburgh, PA, 1998.
- (15) Curtiss, L. A.; Raghavachari, K.; Redfern, P. C.; Pople, J. A. *J. Chem. Phys.* **1997**, *106*, 1063.
- (16) <http://webbook.nist.gov>.
- (17) Nicolaidis, A.; Rauk, A.; Glukhovstev, M. N.; Radom, L. *J. Phys. Chem.* **1996**, *100*, 17460.
- (18) Baer, T.; Hase, W. L. *Unimolecular reactions Dynamics*; Oxford University Press: Oxford, U.K., 1996.
- (19) Chesnavich, W. J.; Bowers, M. T. *Gas-Phase Ion Chemistry*; Bowers, M. T., Ed.; Academic Press: New York, 1979; Vol. 1, pp 119–151.
- (20) Chesnavich, W. J.; Bass, L.; Grice, M. E.; Song, K.; Webb, D. A. *QCPE* **1988**, *8*, 557.